CENP-C is a blueprint for constitutive centromere–associated network assembly within human kinetochores

Kerstin Klare,[1]* John R. Weir,[1]* Federica Basilico,[1,3] Tomasz Zimniak,[4] Lucia Massimiliano,[3] Nina Ludwigs,[2] Franz Herzog,[4] and Andrea Musacchio[1,5]

[1]Department of Mechanistic Cell Biology and [2]Department of Structural Biochemistry, Max Planck Institute of Molecular Physiology, 44227 Dortmund, Germany
[3]Department of Experimental Oncology, European Institute of Oncology, 20139 Milan, Italy
[4]Gene Center Munich, Ludwig-Maximilians-Universität München, 81377 Munich, Germany
[5]Centre for Medical Biotechnology, Faculty of Biology, University Duisburg-Essen, 45141 Essen, Germany

Kinetochores are multisubunit complexes that assemble on centromeres to bind spindle microtubules and promote faithful chromosome segregation during cell division. A 16-subunit complex named the constitutive centromere–associated network (CCAN) creates the centromere–kinetochore interface. CENP-C, a CCAN subunit, is crucial for kinetochore assembly because it links centromeres with the microtubule-binding interface of kinetochores. The role of CENP-C in CCAN organization, on the other hand, had been incompletely understood. In this paper, we combined biochemical reconstitution and cellular investigations to unveil how CENP-C promotes kinetochore targeting of other CCAN subunits. The so-called PEST domain in the N-terminal half of CENP-C interacted directly with the four-subunit CCAN subcomplex CENP-HIKM. We identified crucial determinants of this interaction whose mutation prevented kinetochore localization of CENP-HIKM and of CENP-TW, another CCAN subcomplex. When considered together with previous observations, our data point to CENP-C as a blueprint for kinetochore assembly.

Introduction

Accurate and timely chromosome segregation in mitosis and meiosis is essential for cellular and organismal viability. During mitosis, sister chromatids generated upon DNA replication retain cohesion until they are bioriented on the mitotic spindle. Release of sister chromatid cohesion at the metaphase-to-anaphase transition allows the spindle to separate the sister chromatids into two genetically identical daughter cells (Cheerambathur and Desai, 2014).

Kinetochores mediate the attachment of sister chromatids to spindle microtubules. These large structures, consisting of several copies of ∼30 core subunits, become established on a segment of specialized chromatin named the centromere, whose main hallmark is the presence of the histone H3 variant CENP-A (or CenH3; Fig. 1 A; McAinsh and Meraldi, 2011; Fukagawa and Earnshaw, 2014). At low resolution, kinetochores appear as laminar structures, with an outer plate receiving the ends of spindle microtubules, and an inner plate adjacent to dense centromeric chromatin (Santaguida and Musacchio, 2009; Cheeseman, 2014). The outer kinetochore plate hosts the KMN (Knl1 complex, Mis12 complex, Ndc80 complex) network, a 10-subunit assembly that plays a crucial role as a receptor for microtubules (Cheeseman et al., 2006; DeLuca et al., 2006). The inner kinetochore hosts the constitutive centromere–associated network (CCAN), a complex of at least 16 different CENPs (centromeric proteins), several of which were originally identified in the CENP-A interactome of vertebrates (McCleland et al., 2004; Obuse et al., 2004; Foltz et al., 2006; Izuta et al., 2006; Okada et al., 2006; Hori et al., 2008).

A subset of CCAN subunits, including CENP-N, the CENP-TW complex, and CENP-C, have been recognized as potential "founders" of kinetochore assembly downstream of CENP-A (Fig. 1 A; Hori et al., 2008, 2013; Carroll et al., 2009, 2010; Gascoigne et al., 2011; Guse et al., 2011; Kato et al., 2013). In vitro, CENP-N has been shown to interact directly with CENP-A nucleosomes (Carroll et al., 2009). Chl4, the CENP-N orthologue in *Saccharomyces cerevisiae*, additionally binds tightly to Iml3 (orthologous to CENP-L; Guo et al., 2013; Hinshaw and Harrison, 2013). Although functionally poorly characterized, the CENP-LN complex has been shown to bind directly to CENP-C and to require it for kinetochore localization, at least in yeast (Tanaka et al., 2009; Hinshaw

*K. Klare and J.R. Weir contributed equally to this paper.

Correspondence to Andrea Musacchio: andrea.musacchio@mpi-dortmund.mpg.de

Abbreviations used in this paper: CCAN, constitutive centromere–associated network; IRES, internal ribosomal entry site; SEC, size-exclusion chromatography; TCEP, Tris(2-carboxyethyl)phosphine.

The Rockefeller University Press $30.00
J. Cell Biol. Vol. 210 No. 1 11–22
www.jcb.org/cgi/doi/10.1083/jcb.201412028

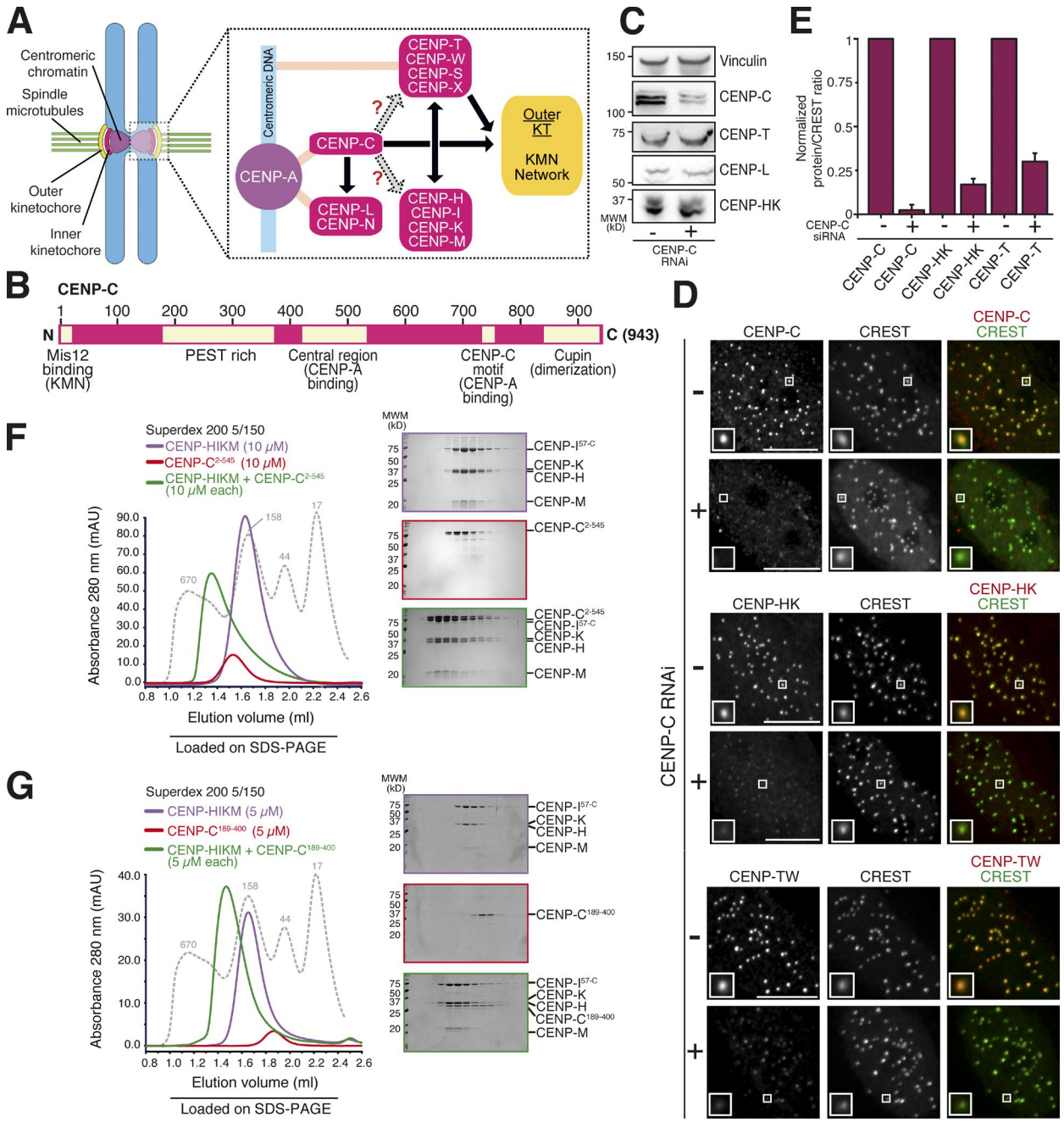

Figure 1. **Depletion of CENP-C abolishes localization of CCAN to kinetochores.** (A) Schematic kinetochore organization. CCAN subunits are shown in hot pink. Light pink lines indicate presumed contacts with centromeric chromatin. Black arrows indicate direct and well-established interactions. Gray arrows represent interactions that are still uncharacterized and that were characterized in this study. For instance, whether localization of CENP-STWX to inner kinetochores requires CENP-C is controversial. Direct interaction of CENP-STWX to CENP-HIKM has been demonstrated recently and reflects in codependency for kinetochore localization. Both CENP-STWX and CENP-C contribute to recruitment of outer kinetochore components. (B) Schematic representation of human CENP-C depicting some of the protein's crucial domains. N, N terminus; C, C terminus. (C) Whole cell protein extracts from Flp-In T-REx HeLa cells treated with control or CENP-C siRNAs were run on SDS-PAGE and immunoblotted for the indicated kinetochore proteins. Vinculin served as a loading control. MWM, molecular weight marker. (D) Representative images showing kinetochore levels of CENP-C, CENP-TW (with an antibody raised against the CENP-TW complex), and CENP-HK (with an antibody raised against the CENP-HK complex) in Flp-In T-REx HeLa cells upon treatment with control and CENP-C siRNA in interphase. Kinetochores were visualized with CREST sera. Upon CENP-C siRNA, CENP-C, CENP-HK, and CENP-TW were displaced from kinetochores. Bars, 10 µm. Magnification = 630×. Insets show a magnification of the white boxed areas that capture one or more kinetochores in each panel. (E) Quantifications are expressed as normalized protein/CREST fluorescence intensity ratios from the experiment in D. Graphs and bars indicate means ± SEM of three independent experiments for CENP-C, CENP-HK, and CENP-TW. (F) SEC elution profile shows CENP-C$^{2–545}$ (~62 kD) elutes earlier than predicted based on its molecular mass, consistent with an unfolded structure. The modest height of the CENP-C peak is caused by low abundance of aromatic amino acids. CENP-C$^{2–545}$ and CENP-HIKM, both at 10 µM, form a stable, apparently stoichiometric complex on an analytical SEC. Shown is the typical outcome of at least five experiments. (G) SEC elution profile of CENP-C$^{189–400}$ (~24 kD) and of its combination with CENP-HIKM, both at 5 µM. Also CENP-C$^{189–400}$ and CENP-HIKM form a stoichiometric complex and coelute in analytical SEC. Shown is the typical outcome of at least three experiments. The gray dotted lines show the elution profile of globular markers of known molecular masses, as indicated.

and Harrison, 2013). In vertebrates, the CENP-LN complex has been shown to contribute to localization of downstream CCAN subunits, including those in the CENP-HIKM complex (Carroll et al., 2009, 2010).

CENP-T and CENP-W are histone fold domain–containing proteins and form a tightly interacting complex (Foltz et al., 2006; Hori et al., 2008). They also interact with two additional histone fold domain proteins named CENP-S and CENP-X (Amano et al., 2009; Nishino et al., 2012). It has been proposed that the CENP-STWX complex may form a specialized centromeric nucleosome-like structure (Nishino et al., 2012), but a recent study suggested that these proteins bind preferentially to internucleosomal linker DNA (Takeuchi et al., 2014). Importantly, the N-terminal region of CENP-T interacts directly, in a phosphorylation-dependent manner, with the Ndc80 subcomplex in the KMN network at the outer kinetochore (Bock et al., 2012; Schleiffer et al., 2012; Malvezzi et al., 2013; Nishino et al., 2013), thus contributing to outer kinetochore assembly. When expressed ectopically on a noncentromeric chromosome site, the N-terminal region of CENP-T supported outer kinetochore assembly independently of other inner kinetochore subunits (Gascoigne et al., 2011; Hori et al., 2013).

CENP-C (943 residues in humans) was among the first human centromere proteins to be discovered (Earnshaw and Rothfield, 1985; Saitoh et al., 1992). Sequence analysis predicts that CENP-C is mostly intrinsically disordered. Near its N terminus, CENP-C contains a binding site for the Mis12 subcomplex of the KMN network (Fig. 1 B; Przewloka et al., 2011; Screpanti et al., 2011; Hornung et al., 2014). Additionally, CENP-C contains two related short motifs that direct it to the CENP-A nucleosome, an interaction believed to be compatible with CENP-N binding (Milks et al., 2009; Carroll et al., 2010; Guse et al., 2011; Kato et al., 2013). Thus, CENP-C, like CENP-T, has the potential to bridge the underlying centromeric chromatin with the outer kinetochore. Finally, the C-terminal region of CENP-C has been shown to mediate dimerization and to promote interactions with CENP-A deposition machinery (Sugimoto et al., 1997; Cohen et al., 2008; Trazzi et al., 2009; Moree et al., 2011; Dambacher et al., 2012; Unhavaithaya and Orr-Weaver, 2013).

The precise localization dependencies of the centromere proximal proteins CENP-C, CENP-N, and CENP-TW are controversial and so is their role in the recruitment of additional CCAN subunits, including those in a four-subunit subcomplex consisting of the CENP-H, CENP-K, CENP-I, and CENP-M subunits (the CENP-HIKM complex), which we have recently characterized (Basilico et al., 2014). It has been shown that depletion of CENP-C in HeLa cells leads to mislocalization of the subunits of the CENP-HIKM complex and of CENP-T (Carroll et al., 2010; Basilico et al., 2014), suggesting that both localize downstream of CENP-C. Furthermore, CENP-T and the CENP-HIKM subunits were shown to be codependent for kinetochore localization (Hori et al., 2008; Gascoigne et al., 2011; Basilico et al., 2014). Other studies, however, did not report effects from CENP-C depletion on kinetochore localization of CENP-I or CENP-T (Liu et al., 2006; Gascoigne et al., 2011). It was therefore proposed that CENP-T may encode a CENP-C–independent pathway of kinetochore assembly downstream of CENP-A (Gascoigne et al., 2011). Here, we provide strong mechanistic insight on the role of CENP-C and identify CENP-C as a blueprint of kinetochore assembly and as the protein that spatially organizes the localization of all other CCAN subunits downstream of CENP-A.

Results and discussion

Depletion of CENP-C disrupts CCAN organization

We used a protocol previously established in our laboratory (Basilico et al., 2014) to achieve substantial CENP-C depletion by RNAi in HeLa cells (Fig. 1 C). By Western blotting, the overall cellular levels of several additional CCAN subunits, including CENP-T, CENP-L, and CENP-HK, appeared unaffected (Fig. 1 C). Conversely, immunofluorescence experiments demonstrated that the kinetochore levels of CENP-C, CENP-HK, and CENP-TW were strongly reduced in CENP-C–depleted cells (Fig. 1, D and E). These experiments confirm evidence from our and other laboratories that CENP-TW complex localization to kinetochores requires CENP-C (Carroll et al., 2010; Basilico et al., 2014; Kim and Yu, 2015; Krizaic et al., 2015; Logsdon et al., 2015; Tachiwana et al., 2015). Our evidence that CENP-C is required for correct localization of CENP-HK is also consistent with previous studies (Milks et al., 2009; Carroll et al., 2010; Gascoigne et al., 2011). These results, when considered together with evidence that the subunits of the CENP-HIKM complex are required for localization of CENP-TW (Hori et al., 2008; Basilico et al., 2014), suggest that the CENP-TW complex may not create a CENP-C–independent pathway of kinetochore assembly downstream of CENP-A (Gascoigne et al., 2011).

CENP-HIKM and CENP-C interact directly

To investigate whether the observed dependency of the CENP-HIKM complex on CENP-C reflected a direct interaction, we built recombinant versions of CENP-HIKM (Basilico et al., 2014) and CENP-C. We did not observe binding of CENP-HIKM to CENP-C constructs encompassing the majority of the C-terminal region (CENP-$C^{632–943}$; unpublished data). Conversely, recombinant CENP-$C^{2–545}$ (Fig. S1 A) coeluted in a stoichiometric complex with the CENP-HIKM complex from a Superdex 200 size-exclusion chromatography (SEC) column, which separates proteins based on size and shape (Fig. 1 F).

CENP-$C^{2–545}$ contains a Mis12 binding motif (Przewloka et al., 2011; Screpanti et al., 2011), a region rich in proline, glutamate, serine, and threonine (PEST in single letter amino acid code) and therefore referred to as "PEST rich" (Cohen et al., 2008), and a kinetochore targeting domain recently shown to be responsible for a specific interaction with the CENP-A nucleosome (Fig. 1 B; Yang et al., 1996; Song et al., 2002; Fachinetti et al., 2013; Kato et al., 2013). We asked whether the PEST domain was involved in CENP-HIKM binding. Indeed, recombinant CENP-$C^{189–400}$ (essentially limited to the PEST domain; Fig. S1 B) was sufficient to interact with CENP-HIKM in the SEC assay (Fig. 1 G). Thus, CENP-C and CENP-HIKM bind directly, and the PEST region of CENP-C is sufficient for this interaction in vitro.

Characterization of the CENP-C–CENP-HIKM interaction

Next, we tried to identify which subunits of the CENP-HIKM complex might be involved in the interaction with CENP-C. To this end, we immobilized a GST–CENP-$C^{2–545}$ fusion protein to glutathione beads and used it as bait in pull-down assays with CENP-M, the CENP-HK complex, and CENP-$I^{57–281}$ (full-length CENP-I could not be produced because it is not soluble in the absence of CENP-M and CENP-HK; Basilico et al., 2014). Neither CENP-M nor CENP-$I^{57–281}$ bound the

GST–CENP-C$^{2–545}$ bait (Fig. 2 A). In contrast, the CENP-HK complex bound the GST–CENP-C$^{2–545}$ bait (Fig. 2 B) and also the GST–CENP-C$^{189–400}$ bait (Fig. 2 C), indicating that the CENP-HK subcomplex is sufficient for a tight interaction with CENP-C. We conclude that the PEST-rich domain of CENP-C and the CENP-HK subunits of the CENP-HIKM complex are the main determinants of the interaction of CENP-C with the CENP-HIKM complex.

Further characterization of the CENP-C–CENP-HK interaction

To further characterize the interaction of CENP-C with CENP-HK, we subjected the CENP-C$^{2–545}$–CENP-HK complex to cross-linking with the bifunctional reagent BS2G (bis[sulfosuccinimidyl]glutarate), which cross-links the primary amines of lysine side chains within a distance compatible with the length of the cross-linker (7.7 Å; Maiolica et al., 2007; Herzog et al., 2012). Subsequent mass spectrometry analysis identified numerous cross-links between CENP-C and CENP-HK, the majority of which mapped to the PEST domain of CENP-C (Fig. 2 D and Table S1), in agreement with the binding assays discussed in the previous paragraph.

Low average representation of hydrophobic residues is a defining feature of intrinsically disordered proteins. Within such proteins, however, binding sites for interacting partners often coincide with short stretches of hydrophobic and aromatic amino acids. We noticed that two closely spaced lysine residues (K271 and K273), which were identified as hotspots in the cross-linking experiments, flank a Leu-Phe-Leu motif (residues 265–267) that appears to be conserved in evolution (Fig. 2 E). A second conserved hydrophobic/aromatic motif (residues 317–320) was also identified. Interestingly, both the Leu-Phe-Leu motif and the second motif appear to be present in Mif2p, the *S. cerevisiae* homologue of CENP-C, but in Mif2p their relative position is swapped.

To test a possible role of the CENP-C hydrophobic motifs in the interaction with the CENP-HIKM complex, we initially divided the CENP-C PEST region in two separate constructs of approximately similar length (CENP-C residues 189–290 and 290–400) each containing only one of the two hydrophobic motifs. As immobilized GST fusion proteins, both CENP-C constructs were sufficient for an interaction with the CENP-HIKM complex in pull-down assays (Fig. 2, F and G), suggesting that the binding site for CENP-HK on CENP-C is extended, as already suggested by the cross-linking experiments.

We therefore tested the effects of mutations in the individual hydrophobic motifs of CENP-C. To this end, we created a triple alanine mutant of residues Leu265, Phe266, and Leu267 (henceforth referred to as "3A" mutant) on the GST–CENP-C$^{189–290}$ construct (GST–CENP-C$^{189–290\text{-}3A}$) as well as a single alanine mutant at residues Trp317 (W317A) on the CENP-C$^{290–400}$ construct (CENP-C$^{290–400\text{-}W317A}$). Both mutants prevented the interaction of their cognate CENP-C segment with CENP-HIKM, clearly implicating the mutated CENP-C residues in the interaction (Fig. 2, F and G). On the other hand, mutations in a highly conserved Glu-Phe-Ile-Ile-Asp motif at residues 302–306 of CENP-C did not interfere with the interaction with CENP-HK (Fig. S2, A and B).

We then combined the mutations (henceforth referred to as "4A" mutant) in the context of the GST–CENP-C$^{2–545}$ construct (GST–CENP-C$^{2–545\text{-}4A}$) and tested their effects on CENP-HIKM binding. Although neither mutation grossly perturbed CENP-HIKM binding in isolation (unpublished data), their combination disrupted CENP-HIKM binding (Fig. 2 H), confirming the importance of both hydrophobic motifs in the CENP-C PEST region on the interaction with CENP-HIKM. In SEC experiments, binding of CENP-C$^{2–545\text{-}3A}$ or CENP-C$^{2–545\text{-}W317A}$ to CENP-HIKM was partially impaired, whereas the combination of mutations in the CENP-C$^{2–545\text{-}4A}$ mutant entirely prevented binding to CENP-HIKM (Fig. S1, C–F), demonstrating that the mutations have additive negative effects on the physical interaction of the CENP-HIKM complex and CENP-C. The interaction of CENP-C$^{2–545\text{-}4A}$ with the Mis12 complex (Petrovic et al., 2010, 2014; Screpanti et al., 2011), which involves the N-terminal region of CENP-C (Fig. 1 B), appeared unaltered in comparison to wild-type CENP-C$^{2–545}$ (Fig. S3, A–E).

The CENP-C–CENP-HIKM interaction promotes CENP-HIKM localization to kinetochores

We asked whether the CENP-HIKM binding interface of CENP-C is important for kinetochore localization of CCAN subunits in HeLa cells. For this, we generated inducible stable cell lines that expressed full-length wild-type GFP–CENP-C, or the 3A, W317A, or 4A mutants (Fig. S3, F and G). After depletion of endogenous CENP-C by RNAi and induction of transgene expression, the levels of CENP-HK at kinetochores were quantified (Fig. 3 A). Expression of GFP–CENP-C^{wt} largely rescued the kinetochore levels of CENP-HK observed in control cells. GFP–CENP-C^{3A} and GFP–CENP-C^{W317A}, on the other hand, only produced a partial rescue of the kinetochore levels of CENP-HK (Fig. 3 A), in agreement with their partial retention of the interaction with CENP-HIKM observed in SEC experiments (Fig. S1, C–F). Conversely, GFP–CENP-C^{4A} was unable to produce significant rescue of the CENP-HK levels (Fig. 3, A and B), in line with the biochemical experiments.

These results were supported by immunoprecipitation experiments in which we used GFP–CENP-C$^{1–544\text{-}wt}$ or GFP–CENP-C$^{1–544\text{-}4A}$ as baits (we did not use full-length CENP-C for these experiments to avoid dimerization with endogenous CENP-C via the CENP-C C-terminal domain). GFP–CENP-C$^{1–544\text{-}wt}$ efficiently pulled down CENP-HK, whereas GFP–CENP-C$^{1–544\text{-}4A}$ failed to do so (Fig. 3 C). Overall, the remarkable consistency of the results of experiments in vitro and in vivo allows us to conclude that CENP-HIKM binds directly to CENP-C and that this interaction is required for kinetochore localization of CENP-HIKM.

CENP-TW localization to kinetochores depends on HIKM

In Fig. 1 (D and E), we demonstrated that kinetochore localization of CENP-TW depends on CENP-C. Kinetochore localization of CENP-TW had been previously shown to depend also on the CENP-HIKM complex (Hori et al., 2008; Basilico et al., 2014). Thus, we analyzed how CENP-C mutants impairing CENP-HIKM localization to kinetochores impacted kinetochore localization of CENP-TW. As for CENP-HK, wild-type CENP-C fully rescued kinetochore localization of CENP-TW, but there was a progressive reduction of CENP-TW kinetochore levels when CENP-C mutants were expressed (Fig. 4, A and B). In agreement with these observations, we readily identified CENP-TW in precipitates of GFP–CENP-C$^{1–544\text{-}wt}$ but not in precipitates of GFP–CENP-C$^{1–544\text{-}4A}$ (Fig. 3 C).

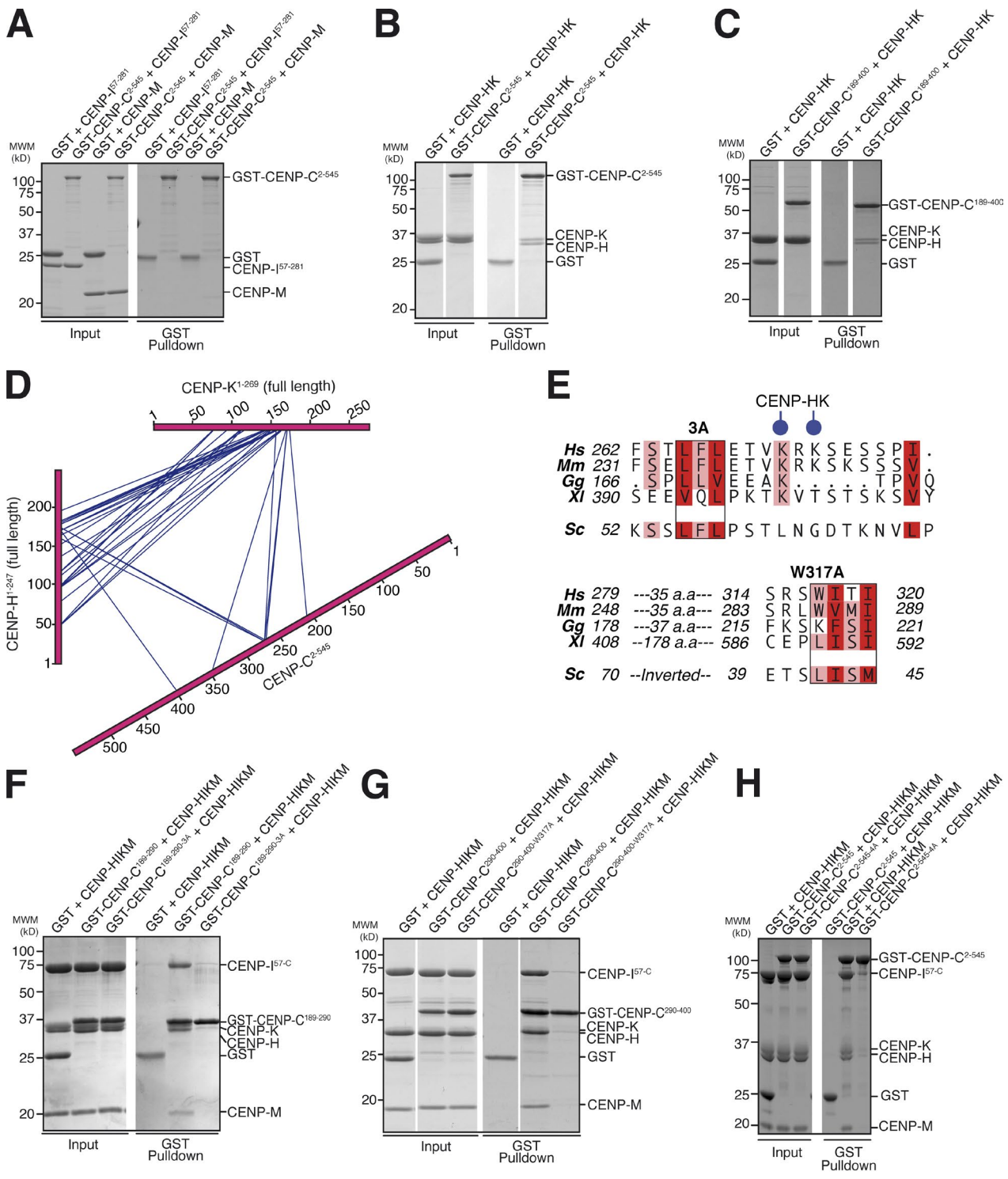

Figure 2. **Characterization of the CENP-C–CENP-HIKM interaction.** (A) GST pull-down assay of GST–CENP-$C^{2–545}$ with CENP-M or CENP-$I^{57–281}$. CENP-C does not bind to CENP-M or CENP-$I^{57–281}$ in this assay. (B) GST pull-down assay of GST–CENP-$C^{2–545}$ with CENP-HK. (C) GST pull-down assay of GST–CENP-$C^{189–400}$ with CENP-HK. In B and C, CENP-$C^{2–545}$ and CENP-$C^{189–400}$, respectively, bind to CENP-HK. (D) Summary of cross-links within the CENP-$C^{2–545}$–CENP-HK complex. Intermolecular cross-links are shown in blue. Intramolecular cross-links are not shown but are listed in Table S1. CENP-HK binds to CENP-C within its PEST-rich domain. (E) Within the boxed regions are two conserved hydrophobic motifs in CENP-$C^{189–400}$. In the 3A mutant, L265, F266A, and L267A were mutated to alanine. The 4A mutant combines 3A with W317A. Two Lys residues found to cross-link with CENP-HK are shown with blue circles. Budding yeast Mif2 is shown for comparison. Curiously, the regions conserved in Mif2 seem to be inverted. *Hs*, *Homo sapiens*; *Mm*, *Mus musculus*; *Gg*, *Gallus gallus*; *Xl*, *X. laevis*; *Sc*, *S. cerevisiae*. Red and pink boxes indicate positions in the CENP-C sequence that are either fully conserved (per residue class, e.g., hydrophobic and aromatic) or conserved in at least four in five sequences, respectively. (F) GST–CENP-$C^{189–290-3A}$ was unable to bind HIKM in a GST pull-down assay, in contrast to wild-type CENP-$C^{189–290}$. (G) GST–CENP-$C^{290–400-W317A}$ was unable to bind HIKM in a GST pull-down assay, in contrast to wild-type GST–CENP-$C^{290–400}$. (H) GST pull-down assay of GST–CENP-$C^{2–545}$ shows binding to HIKM, whereas GST–CENP-$C^{2–545-4A}$ is effectively impaired in HIKM binding. White lines indicate that intervening lanes have been spliced out. MWM, molecular weight marker.

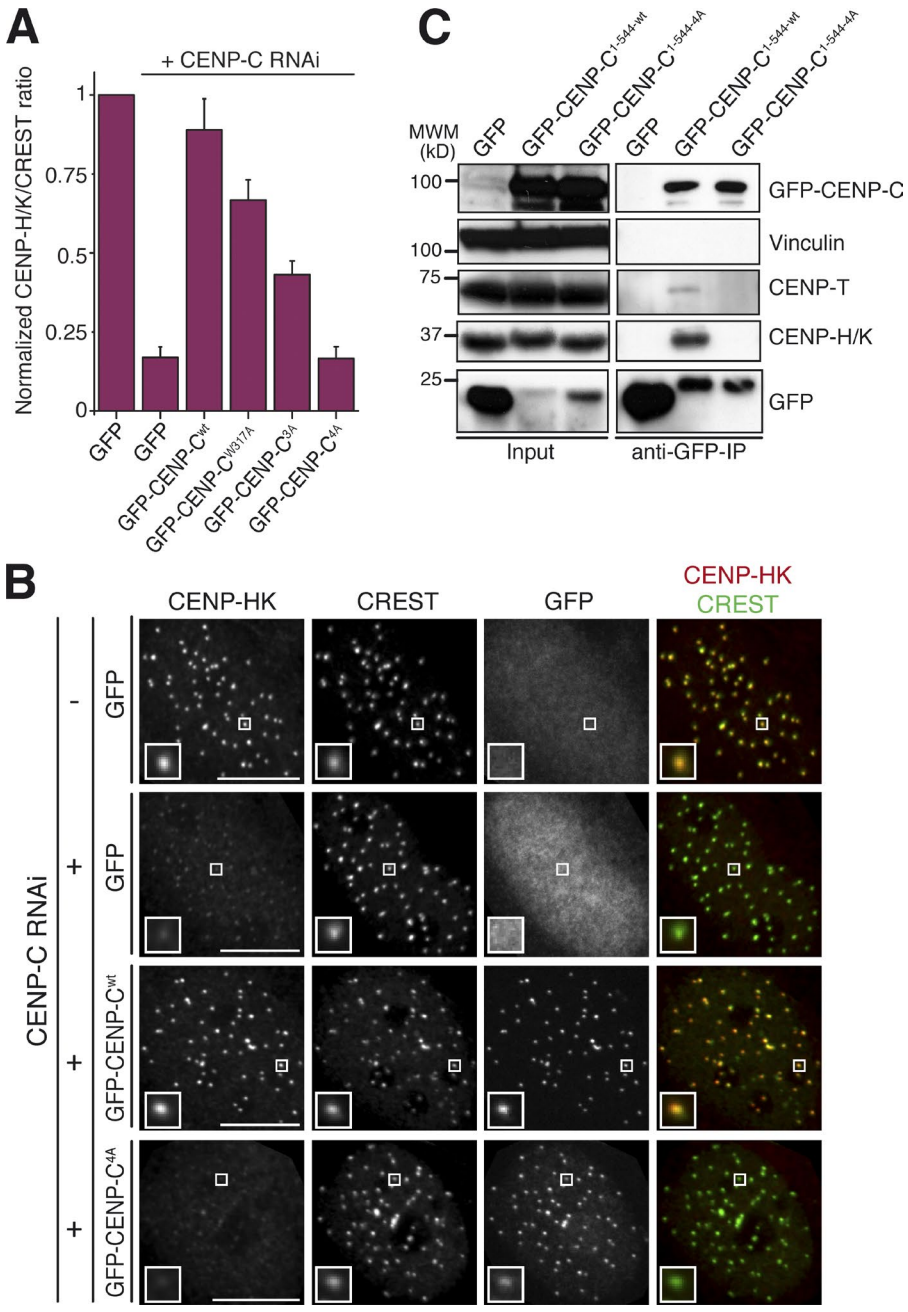

Figure 3. **The CENP-C^{4A} mutant abrogates rescue of CENP-HK localization to kinetochores.** (A) Quantification of immunofluorescence experiment in fixed Flp-In T-REx HeLa cells depleted of endogenous CENP-C (where indicated) and expressing the indicated GFP constructs. The kinetochore levels of CENP-HK were measured and normalized to CREST. Graphs and bars indicate means ± SEM of three independent experiments. (B) Representative images of the dataset quantified in A and documenting the levels of CENP-HK protein in cells expressing GFP–CENP-C or GFP–CENP-C^{4A}. Bars, 10 µM. Magnification = 630×. Insets show a magnification of the white boxed areas that capture one or more kinetochores in each panel. (C) GFP–CENP-C$^{1–544}$ but not the GFP–CENP-C$^{1–544-4A}$ mutant coimmunoprecipitates CENP-HK and CENP-TW. α-GFP coimmunoprecipitation analysis was performed on protein extracts from cycling Flp-In T-REx HeLa cells expressing GFP, GFP–CENP-C, or GFP–CENP-C^{4A} from an inducible promoter. Total protein extracts (Input) and immunoprecipitates (α-GFP co-IP) were separated by SDS-PAGE and blotted with the indicated antibodies. Vinculin served as loading control. IP, immunoprecipitation.

GST–CENP-C$^{2–545}$ did not interact with CENP-TW in a pull-down assay with recombinant proteins (Fig. 4 C). In contrast, CENP-TW was pulled down by GST–CENP-C$^{2–545}$ when CENP-HIKM was included in the reaction (Fig. 4 C), in agreement with our previous results showing a direct interaction of CENP-HIKM with CENP-TW (Basilico et al., 2014). The result was confirmed by Western blot analysis of immunoprecipitated fractions (Fig. 4 C). Although these data argue that CENP-HIKM is necessary for kinetochore recruitment of CENP-TW (Basilico et al., 2014), the interaction of CENP-HIKM with CENP-TW in vitro appears to be relatively low affinity in comparison with the very robust interaction of CENP-HIKM with CENP-C. This predicts that CENP-TW may require additional contacts for efficient kinetochore targeting. Collectively, the localization and interaction results, including the observation that CENP-HIKM and CENP-TW are direct interaction partners (Basilico et al., 2014), support the conclusion that both CENP-HIKM and CENP-TW depend on CENP-C for kinetochore localization and that CENP-TW does not bind tightly to CENP-C, at least in the absence of other interaction partners.

Conclusions

The CCAN has been implicated in the fascinating mechanism of new CENP-A deposition during the cell cycle, a process that is at the basis of epigenetic inheritance of centromeres (Fukagawa and Earnshaw, 2014). Moreover, the inner kinetochore is directly involved in recruiting, shaping, and functionally influencing the outer kinetochore (Schittenhelm et al., 2007; Ribeiro et al., 2010; Gascoigne et al., 2011; Przewloka et al., 2011; Screpanti et al., 2011; Matson et al., 2012; Hori et al., 2013; Hornung et al., 2014; Suzuki et al., 2014). Finally, the CCAN has been implicated in interactions with the microtu-

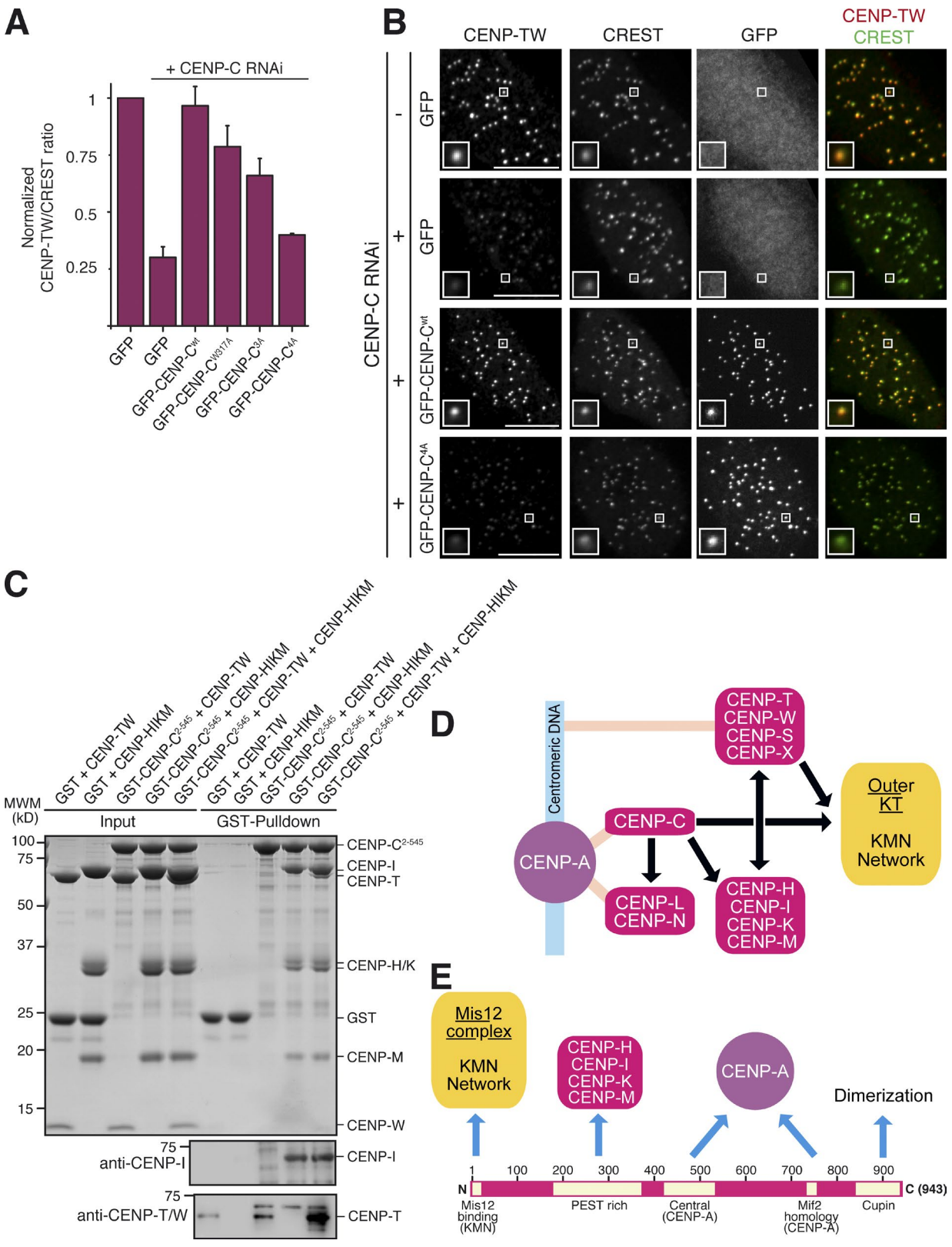

Figure 4. **CENP-C^{4A} abrogates rescue of CENP-TW localization to kinetochores.** (A) Quantification of immunofluorescence experiment in fixed Flp-In T-REx HeLa cells depleted of endogenous CENP-C (where indicated) and expressing the indicated GFP constructs. The kinetochore levels of CENP-TW were measured and normalized to CREST. Graphs and bars indicate mean ± SEM of three independent experiments. (B) Representative images of the dataset quantified in A and documenting the levels of CENP-TW protein in cells expressing GFP–CENP-C or GFP–CENP-C^{4A}. Bars, 10 µM. Magnification = 630×. (C) GST–CENP-C$^{2–545}$ does not bind directly to CENP-TW in a GST pull-down assay. Bands were visualized with Coomassie brilliant blue staining. (left) Only when HIKM is included in the assay, CENP-TW is incorporated into the complex. Because CENP-I and CENP-T comigrate on the SDS-PAGE gel

bule plus end, thus possibly complementing the function of the outer kinetochore in chromosome alignment (McClelland et al., 2007; Amaro et al., 2010; Dumont et al., 2012). Understanding the physical organization of the inner kinetochore is therefore an important goal of current kinetochore research. Here, we have identified the PEST domain of CENP-C as an interaction domain for the CENP-HIKM complex and implicated four conserved residues of CENP-C in this interaction. Mutation of these residues impairs binding of CENP-C to CENP-HIKM (but not to the Mis12 complex) in vitro to undetectable levels and leads to a complete loss of CENP-HIKM kinetochore localization in vivo. The same mutations on CENP-C also lead to a dramatic loss of CENP-TW from kinetochores, which is consistent with our previous observation that CENP-TW binds the CENP-HIKM complex directly (Basilico et al., 2014). N-terminal or C-terminal tagging of CENP-C interfered with kinetochore recruitment of the Mis12 complex or with stable incorporation of CENP-C to kinetochores, respectively, preventing us from testing rigorously the effects of the four CENP-C mutations on kinetochore recruitment of the Mis12 complex (unpublished data). However, our results in vitro and previous evidence (Basilico et al., 2014; Kim and Yu, 2015) argue that depletion of HIKM subunits is not sufficient for robust displacement of the Mis12 complex from kinetochores.

Our results are consistent with a model in which CENP-C occupies the first position downstream of CENP-A in a single pathway of kinetochore assembly (Fig. 4 D). Our data argue that CENP-TW positions itself in this pathway, together with other CCAN subunits, downstream of CENP-C, in agreement with several other studies (Carroll et al., 2010; Basilico et al., 2014; Kim and Yu, 2015; Krizaic et al., 2015; Logsdon et al., 2015; Tachiwana et al., 2015). Claims that CENP-T and CENP-C establish independent pathways of kinetochore recruitment downstream from CENP-A (Gascoigne et al., 2011; Rago et al., 2015) may reflect differences in the levels of RNAi-based depletion or in the details of the localization analysis. Several CCAN subunits have been implicated in the deposition of new CENP-A required for centromere propagation (see for instance Okada et al., 2009; Moree et al., 2011; Fachinetti et al., 2013). This is a potential confounding factor because the localization pattern of inner kinetochore proteins cannot be solely viewed as a representation of a static set of protein–protein interactions. Interference with new CENP-A deposition during each cell cycle will eventually affect indirectly the pattern of localization of inner kinetochore subunits, regardless of their direct physical interactions. Be that as it may, our conclusion that CENP-T is positioned downstream of CENP-C is not inconsistent with the identified role of CENP-T in regulating outer kinetochore assembly through an interaction with the Ndc80 complex and possibly other outer kinetochore components (Gascoigne et al., 2011; Bock et al., 2012; Schleiffer et al., 2012; Nishino et al., 2012, 2013; Malvezzi et al., 2013; Kim and Yu, 2015; Rago et al., 2015). The conclusion, however, implies that such role of CENP-TW in kinetochore assembly occurs downstream of CENP-C (Fig. 4 D).

Dissection of CENP-C is bringing to light a linear organization of binding motifs within a largely structurally disordered protein (Fig. 4 E). Specifically, the N-terminal region and the central domain have been shown to interact with the outer kinetochore and the centromere, respectively (Przewloka et al., 2011; Screpanti et al., 2011; Kato et al., 2013; Hornung et al., 2014), whereas the C-terminal region contains binding sites for proteins involved in new CENP-A deposition and CENP-C dimerization (Sugimoto et al., 1997; Cohen et al., 2008; Trazzi et al., 2009; Moree et al., 2011; Dambacher et al., 2012; Unhavaithaya and Orr-Weaver, 2013). We now report that between the outer kinetochore binding site and the CENP-A binding site is a binding site for the CCAN subunits CENP-HIKM. This linear organization of motifs (Fig. 4 E) justifies our interpretation that CENP-C may be a blueprint that determines the correct positioning of kinetochore subunits along the inner to outer kinetochore axis (Suzuki et al., 2014). In the future, it will be important to elucidate the entire network of interactions of CCAN subunits around the CENP-C scaffold through biochemical reconstitution and in vivo validation.

Materials and methods

Expression and purification of CENP-C constructs

From a codon-optimized cDNA synthesized by GeneArt (Life Technologies) encoding the human CENP-C sequence, different CENP-C constructs have been subcloned in pGEX-6P-2rbs (GenBank accession code KM817768), a modified pGEX-6P vector (GE Healthcare; the vector utilizes an inducible *tac* promoter), as a 3′ fusion to the sequence encoding GST. Mutant CENP-C constructs were created by site-directed mutagenesis using the QuikChange kit (Agilent Technologies). All constructs and mutants were sequence verified. The expression and purification procedure was the same for all CENP-C constructs and mutants. The parental pGEX-6P-2rbs vector expressing CENP-$C^{2–545}$ was a gift of S. Jeganathan (Max-Planck Institute of Molecular Physiology, Dortmund, Germany). *Escherichia coli* C41 (DE3) cells harboring vectors expressing CENP-C constructs or CENP-C mutant constructs were grown in Terrific Broth at 37°C to an OD600 of 0.8–1, when 0.2 mM IPTG was added and the culture was grown at 20°C for ∼15 h. Cell pellets were resuspended in lysis buffer (50 mM Hepes, pH 7.5, 500 mM NaCl, 10% glycerol, and 2 mM β-mercaptoethanol), lysed by sonication, and cleared by centrifugation at 48,000 *g* at 4°C for 30 min. The cleared lysate was applied to glutathione Sepharose 4 Fast Flow beads (GE Healthcare) preequilibrated in lysis buffer, incubated at 4°C for 2 h, washed with 70 column volumes of lysis buffer and either subjected to an overnight cleavage reaction with 3C protease to separate CENP-C constructs from GST or eluted in a lysis buffer supplemented with 20 mM glutathione. A 5-ml HiTrap Heparin HP column (GE Healthcare) was preequilibrated in 20 mM Hepes, pH 7.5, 200 mM NaCl, 5% glycerol, and 2 mM β-mercaptoethanol. The eluate from glutathione beads was adjusted to a final salt concentration of 200 mM NaCl, loaded onto the Heparin column, and eluted with a linear gradient of 200–1,200 mM NaCl in 20 bed column volumes. Fractions containing CENP-C were concentrated and loaded onto a Superdex 200 SEC column (GE Healthcare) preequilibrated in SEC buffer (20 mM Hepes, pH 7.5, 300 mM NaCl, 2.5% glycerol, and 2 mM Tris(2-carboxyethyl) phosphine [TCEP]). Fractions containing CENP-C were concentrated, flash frozen in liquid nitrogen, and stored at −80°C.

shown, 10% of the pull-down samples were separated on a new SDS-PAGE and subjected to Western blotting with either a CENP-T or CENP-I antibody. (D) Recasting of the kinetochore assembly scheme based on our new results. (E) The CENP-C sequence contains a linear array of motifs whose succession appears to correlate with the order of kinetochore assembly from the CENP-A nucleosome toward the outer kinetochore. N, N terminus; C, C terminus.

GST pull-down assays

All GST pull-down experiments were performed using preblocked GSH Sepharose beads in pull-down buffer (10 mM Hepes, pH 7.5, 200 mM NaCl, 0.05% Triton X-100, 2.5% glycerol, and 1 mM TCEP). GST–CENP-C various constructs always served as bait at a 1-µM concentration, whereas potential binding partners served as prey at a 3-µM concentration. The bait was loaded to 12-µl preblocked beads, before the prey was added. At the same time, 1 µg of each protein was added into Laemmli sample loading buffer for the input gel. The reaction volume was added up to 40 µl with buffer and incubated at 4°C for 1 h, rotating. Beads were spun down at 500 *g* for 3 min. The supernatant was removed, and beads were washed twice with 250 µl buffer. The supernatant was removed completely, and samples were boiled in 15 µl Laemmli sample loading buffer and run on a 14% SDS-PAGE gel. Bands were visualized with Coomassie brilliant blue staining.

Preblocking of GSH Sepharose beads

750 µl GSH Sepharose beads were washed twice with 1 ml washing buffer (20 mM Hepes, pH 7.5, and 200 mM NaCl) and incubated in 1 ml blocking buffer (20 mM Hepes, pH 7.5, 500 mM NaCl, and 500 µg/µl BSA) overnight at 4°C rotating. Beads were washed 5× with 1 ml washing buffer and resuspended in 500 µl washing buffer to have a 50/50 slurry of beads and buffer.

Analytical SEC migration shift assays

Analytical SEC experiments were performed on a calibrated Superdex 200 5/150 column (GE Healthcare). All samples were eluted under isocratic conditions at 4°C in SEC buffer (20 mM Hepes, pH 7.5, 300 mM NaCl, 2.5% glycerol, and 2 mM TCEP) at a flow rate of 0.2 ml/min. Elution of proteins was monitored at 280 nm. 100-µl fractions were collected and analyzed by SDS-PAGE and Coomassie blue staining. To detect the formation of a complex, proteins were mixed at the indicated concentrations in 50 µl, incubated for at least 2 h on ice, and then subjected to SEC.

Cross-linking analysis

CENP-C$^{2–545}$–CENP-H–CENP-K complex was cross-linked with isotope-labeled disuccinimidyl suberate and digested with Lys-C and trypsin after quenching with ammonium bicarbonate. Cross-linked peptides were enriched using SEC, analyzed by liquid chromatography coupled to tandem mass spectrometry, and identified by the search algorithm, xQuest. Cross-linking, mass spectrometry analysis, and database searching were performed as previously described (Herzog et al., 2012).

Visualization of the cross-links was performed by converting the raw data (in form of Excel spreadsheets) to the GEXF (Graph Exchange XML Format) data format using custom shell scripts (supplemental material). The data were then imported into the Gephi software that was modified to allow simultaneous calculation and display of curved and straight connectors (i.e., intra- and intermolecular cross-links). The Gephi graph was exported as an Illustrator file (Adobe) for final processing.

Cell culture and transfection

Parental Flp-In T-REx HeLa cells used to generate stable doxycycline-inducible cell lines were a gift from S. Taylor (University of Manchester, Manchester, England, UK). They were grown at 37°C in the presence of 5% CO_2 in DMEM (PAN Biotech) supplemented with 10% tetracycline-free FBS (Invitrogen) and 2 mM L-glutamine (PAN-Biotech). Flp-In T-REx HeLa cells (Tighe et al., 2004) and maintained in DMEM supplemented with 10% tetracycline-free FBS, 2 mM L-glutamine, 250 µg/ml hygromycin (Invitrogen), and 4 µg/ml blasticidin (Invitrogen). GFP–CENP-C fusions were expressed by addition of 25 ng/ml doxycycline (Sigma-Aldrich) for 24 or 48 h. For CENP-C silencing, we used a single siRNA (target sequence: 5′-GGAUCAUCUCAGAAUAGAA-3′ obtained from Sigma-Aldrich), targeting the coding region of endogenous CENP-C mRNA. Transfections were performed with HyPerFect (QIAGEN) according to the manufacturer's instructions. To obtain an efficient depletion of CENP-C, 60 nM siRNA was transfected 3× within 72 h. In the last 24 h, 25 ng/ml doxycycline was added to induce GFP–CENP-C construct expression. The siRNA did not affect expression of GFP-CENP. Phenotypes were analyzed 96 h after the first siRNA addition, and protein depletion was monitored by Western blotting or immunofluorescence.

Mammalian plasmids

CENP-C constructs were created by cDNA subcloning in pcDNA5/FRT/TO-EGFP-IRES vector, a modified version of pcDNA5/FRT/TO vector (Invitrogen). pcDNA5/FRT/TO vector (Invitrogen) is a tetracycline-inducible expression vector designed for use with the Flp-In T-REx system. It carries a hybrid human cytomegalovirus/TetO2 promoter for high-level, tetracycline-regulated expression of the target gene. The control plasmid for EGFP expression was created by PCR amplifying the EGFP sequence from pEGFP-C1 (Takara Bio Inc.) and cloning it into the pcDNA5/FRT/TO vector previously modified to carry an internal ribosomal entry site (IRES) sequence to obtain the pcDNA5/FRT/TO EGFP-IRES vector (Petrovic et al., 2010). All plasmids used in the study for mammalian expression (Fig. 3, B and C; and Fig. 4 B) were derived from the pCDNA5/FRT/TO-EGFP-IRES and used for genomic integration and expression of human CENP-C proteins. To create all N-terminally tagged EGFP fusions, we amplified CENP-C full-length or 1–544 fragments by PCR from a full-length human RNAi-resistant CENP-C cDNA synthesized by GeneArt (Life Technologies) and subcloned them in frame with the EGFP tag into the pcDNA5/FRT/TO EGFP-IRES vector using the restriction sites BamHI and XhoI. Mutant CENP-C constructs were created by site-directed mutagenesis using the QuikChange kit (Agilent Technologies). All constructs were sequence verified.

Immunoprecipitation and immunoblotting

Cycling cells were harvested by trypsinization and lysed by incubation in lysis buffer (75 mM Hepes, pH 7.5, 150 mM KCl, 1.5 mM EGTA, 1.5 mM $MgCl_2$, 10% glycerol, 0.075% NP-40, 90 U/ml Benzonase [Sigma-Aldrich], and protease inhibitor cocktail [Serva]) at 4°C for 15 min followed by sonication and centrifugation. Extracts were precleared with a mixture of protein A–Sepharose (CL-4B; GE Healthcare) and protein G–Sepharose (rec-Protein G-Sepharose 4B; Invitrogen) at 4°C for 1 h. Subsequently, extracts were incubated with GFP-Traps (ChromoTek) at 4°C for 3–4 h. Immunoprecipitates were washed with lysis buffer, resuspended in Laemmli sample buffer, boiled, and analyzed by Western blotting using 12% NuPAGE gels (Life Technologies). The following antibodies were used: anti-GFP (in house–made rabbit polyclonal antibody raised against full-length GFP from *Aequorea victoria*, full length; 1:4,000), anti-Vinculin (mouse monoclonal, clone hVIN-1; 1:15,000; V9131; Sigma-Aldrich), anti–α-tubulin (mouse monoclonal, T9026; Sigma-Aldrich), anti–CENP-TW (in house–made rabbit polyclonal antibody SI0882, raised against the full-length protein complex; 1:800; a gift of S. Jeganathan, Max Planck Institute of Molecular Physiology, Dortmund, Germany), anti–CENP-C (rabbit polyclonal antibody SI410 raised against residues 23–410 of human CENP-C; 1:1,200; Trazzi et al., 2009), anti–CENP-HK (rabbit polyclonal antibody SI0930 raised against the full-length human CENP-HK complex; 1:1,000), anti–CENP-I (rabbit polyclonal antibody raised against residues 57–281 of human CENP-I), and anti–CENP-L (rabbit polyclonal, 17007–1-AP; Acries Antibodies). Secondary antibodies were affini-

ty-purified anti–mouse (Amersham, part of GE Healthcare) and anti–rabbit (Amersham) conjugated to horseradish peroxidase (1:10,000). After incubation with ECL Western blotting system (GE Healthcare), images were acquired with ChemiBIS 3.2 (DNR Bio-Imaging Systems). Levels were adjusted with ImageJ (National Institutes of Health) and Photoshop (Adobe), and images were cropped accordingly

Immunofluorescence and quantification

Flp-In T-REx HeLa cells were grown on coverslips precoated with 0.01% poly-L-lysine (Sigma-Aldrich). Cells were fixed with PBS/PHEM (Pipes, Hepes, EGTA, and $MgCl_2$)-paraformaldehyde 4% followed by permeabilization with PBS/PHEM–Triton X-100 0.5%. The following antibodies were used for immunostaining: anti–CENP-TW (in house–made rabbit polyclonal antibody SI0882, raised against the full-length protein complex; 1:800), CREST/anticentromere antibodies (human autoimmune serum, 1:100; Antibodies, Inc.), anti–CENP-C (SI410; 1:1,000), anti–CENP-HK (SI0930; 1:800). Rodamine red–conjugated, DyLight 405–conjugated secondary antibodies were purchased from Jackson ImmunoResearch Laboratories, Inc. Alexa Fluor 647–labeled secondary antibodies were obtained from Invitrogen. Coverslips were mounted with Mowiol mounting media (EMD Millipore). All experiments were imaged at room temperature using the spinning-disk confocal microscopy of a 3i Marianas system (Intelligent Imaging Innovations) equipped with a microscope (Axio Observer Z1; Carl Zeiss), a confocal scanner unit (CSU-X1; Yokogawa Electric Corporation), Plan Apochromat 63× or 100×/1.4 NA objectives (Carl Zeiss), and camera (Orca Flash 4.0 sCMOS; Hamamatsu Photonics) and converted into maximal intensity projections TIFF files for illustrative purposes. Quantification of kinetochore signals was performed on unmodified z series images using Imaris 7.3.4 software (Bitplane). After background subtraction, all signals were normalized to CREST, and values obtained for control cells were set to 1. Quantifications are based on three independent experiments in which 5–10 cells were analyzed.

Online supplemental material

Fig. S1 shows the SEC profiles of two CENP-C segments described in the Results and discussion, as well as SEC profiles demonstrating the compound effects of mutations within the PEST region of CENP-C on the CENP-C–CENP-HIKM interaction. Fig. S2 shows that a conserved Glu-Phe-Ile-Ile-Asp motif of CENP-C is not required for the interaction of CENP-C with CENP-HK. Fig. S3 shows that CENP-$C^{2–545}$ binds the Mis12 complex in SEC experiments even if mutated in the interaction site for CENP-HIKM and loading controls for Figs. 3 and 4 (F and G). Table S1 contains the entire list of intra- and intermolecular cross-links and is provided online as an Excel file. Supplemental material also includes a ZIP file that provides custom scripts used to convert raw cross-linking data from an Excel spreadsheet to the GEXF. Online supplemental material is available at http://www.jcb.org/cgi/content/full/jcb.201412028/DC1. Additional data are available in the JCB DataViewer at http://dx.doi.org/10.1083/jcb.201412028.dv.

Acknowledgments

We thank Giuseppe Ossolengo of the antibody facility at the European Institute of Oncology for help with antibody production, Ingrid Vetter for help with the preparation of Fig. 2 D, Sadasivam Jeganathan for the anti–CENP-TW antibody and the CENP-$C^{2–545}$ construct, Stefano Maffini and Anna De Antoni for help in the development of the CENP-C RNAi protocol, Doro Vogt for preparation of purified CENP-TW protein, and the members of the Musacchio laboratory for helpful discussions.

A. Musacchio acknowledges funding by the European Union's seventh Framework Program European Research Council agreement KINCON and the Integrated Project MitoSys. F. Herzog is supported by the Bavarian Research Center of Molecular Biosystems and by a Ludwigs Maximilian excellent junior grant.

The authors declare no competing financial interests.

Submitted: 5 December 2014
Accepted: 1 June 2015

Amano, M., A. Suzuki, T. Hori, C. Backer, K. Okawa, I.M. Cheeseman, and T. Fukagawa. 2009. The CENP-S complex is essential for the stable assembly of outer kinetochore structure. *J. Cell Biol.* 186:173–182. http://dx.doi.org/10.1083/jcb.200903100

Amaro, A.C., C.P. Samora, R. Holtackers, E. Wang, I.J. Kingston, M. Alonso, M. Lampson, A.D. McAinsh, and P. Meraldi. 2010. Molecular control of kinetochore-microtubule dynamics and chromosome oscillations. *Nat. Cell Biol.* 12:319–329. http://dx.doi.org/10.1038/ncb2033

Basilico, F., S. Maffini, J.R. Weir, D. Prumbaum, A.M. Rojas, T. Zimniak, A. De Antoni, S. Jeganathan, B. Voss, S. van Gerwen, et al. 2014. The pseudo GTPase CENP-M drives human kinetochore assembly. *eLife.* 3:e02978. http://dx.doi.org/10.7554/eLife.02978

Bock, L.J., C. Pagliuca, N. Kobayashi, R.A. Grove, Y. Oku, K. Shrestha, C. Alfieri, C. Golfieri, A. Oldani, M. Dal Maschio, et al. 2012. Cnn1 inhibits the interactions between the KMN complexes of the yeast kinetochore. *Nat. Cell Biol.* 14:614–624. http://dx.doi.org/10.1038/ncb2495

Carroll, C.W., M.C. Silva, K.M. Godek, L.E. Jansen, and A.F. Straight. 2009. Centromere assembly requires the direct recognition of CENP-A nucleosomes by CENP-N. *Nat. Cell Biol.* 11:896–902. http://dx.doi.org/10.1038/ncb1899

Carroll, C.W., K.J. Milks, and A.F. Straight. 2010. Dual recognition of CENP-A nucleosomes is required for centromere assembly. *J. Cell Biol.* 189:1143–1155. http://dx.doi.org/10.1083/jcb.201001013

Cheerambathur, D.K., and A. Desai. 2014. Linked in: formation and regulation of microtubule attachments during chromosome segregation. *Curr. Opin. Cell Biol.* 26:113–122. http://dx.doi.org/10.1016/j.ceb.2013.12.005

Cheeseman, I.M. 2014. The kinetochore. *Cold Spring Harb. Perspect. Biol.* 6:a015826. http://dx.doi.org/10.1101/cshperspect.a015826

Cheeseman, I.M., J.S. Chappie, E.M. Wilson-Kubalek, and A. Desai. 2006. The conserved KMN network constitutes the core microtubule-binding site of the kinetochore. *Cell.* 127:983–997. http://dx.doi.org/10.1016/j.cell.2006.09.039

Cohen, R.L., C.W. Espelin, P. De Wulf, P.K. Sorger, S.C. Harrison, and K.T. Simons. 2008. Structural and functional dissection of Mif2p, a conserved DNA-binding kinetochore protein. *Mol. Biol. Cell.* 19:4480–4491. http://dx.doi.org/10.1091/mbc.E08-03-0297

Dambacher, S., W. Deng, M. Hahn, D. Sadic, J. Fröhlich, A. Nuber, C. Hoischen, S. Diekmann, H. Leonhardt, and G. Schotta. 2012. CENP-C facilitates the recruitment of M18BP1 to centromeric chromatin. *Nucleus.* 3:101–110. http://dx.doi.org/10.4161/nucl.18955

DeLuca, J.G., W.E. Gall, C. Ciferri, D. Cimini, A. Musacchio, and E.D. Salmon. 2006. Kinetochore microtubule dynamics and attachment stability are regulated by Hec1. *Cell.* 127:969–982. http://dx.doi.org/10.1016/j.cell.2006.09.047

Dumont, S., E.D. Salmon, and T.J. Mitchison. 2012. Deformations within moving kinetochores reveal different sites of active and passive force generation. *Science.* 337:355–358. http://dx.doi.org/10.1126/science.1221886

Earnshaw, W.C., and N. Rothfield. 1985. Identification of a family of human centromere proteins using autoimmune sera from patients with scleroderma. *Chromosoma.* 91:313–321. http://dx.doi.org/10.1007/BF00328227

Fachinetti, D., H.D. Folco, Y. Nechemia-Arbely, L.P. Valente, K. Nguyen, A.J. Wong, Q. Zhu, A.J. Holland, A. Desai, L.E. Jansen, and D.W. Cleveland. 2013. A two-step mechanism for epigenetic specification of centromere identity and function. *Nat. Cell Biol.* 15:1056–1066. http://dx.doi.org/10.1038/ncb2805

Foltz, D.R., L.E. Jansen, B.E. Black, A.O. Bailey, J.R. Yates III, and D.W. Cleveland. 2006. The human CENP-A centromeric nucleosome-associated complex. *Nat. Cell Biol.* 8:458–469. http://dx.doi.org/10.1038/ncb1397

Fukagawa, T., and W.C. Earnshaw. 2014. The centromere: chromatin foundation for the kinetochore machinery. *Dev. Cell.* 30:496–508. http://dx.doi.org/10.1016/j.devcel.2014.08.016

Gascoigne, K.E., K. Takeuchi, A. Suzuki, T. Hori, T. Fukagawa, and I.M. Cheeseman. 2011. Induced ectopic kinetochore assembly bypasses the

requirement for CENP-A nucleosomes. *Cell.* 145:410–422. http://dx.doi.org/10.1016/j.cell.2011.03.031

Guo, Q., Y. Tao, H. Liu, M. Teng, and X. Li. 2013. Structural insights into the role of the Chl4-Iml3 complex in kinetochore assembly. *Acta Crystallogr. D Biol. Crystallogr.* 69:2412–2419. http://dx.doi.org/10.1107/S0907444913022397

Guse, A., C.W. Carroll, B. Moree, C.J. Fuller, and A.F. Straight. 2011. In vitro centromere and kinetochore assembly on defined chromatin templates. *Nature.* 477:354–358. http://dx.doi.org/10.1038/nature10379

Herzog, F., A. Kahraman, D. Boehringer, R. Mak, A. Bracher, T. Walzthoeni, A. Leitner, M. Beck, F.U. Hartl, N. Ban, et al. 2012. Structural probing of a protein phosphatase 2A network by chemical cross-linking and mass spectrometry. *Science.* 337:1348–1352. http://dx.doi.org/10.1126/science.1221483

Hinshaw, S.M., and S.C. Harrison. 2013. An Iml3-Chl4 heterodimer links the core centromere to factors required for accurate chromosome segregation. *Cell Reports.* 5:29–36. http://dx.doi.org/10.1016/j.celrep.2013.08.036

Hori, T., M. Amano, A. Suzuki, C.B. Backer, J.P. Welburn, Y. Dong, B.F. McEwen, W.H. Shang, E. Suzuki, K. Okawa, et al. 2008. CCAN makes multiple contacts with centromeric DNA to provide distinct pathways to the outer kinetochore. *Cell.* 135:1039–1052. http://dx.doi.org/10.1016/j.cell.2008.10.019

Hori, T., W.H. Shang, K. Takeuchi, and T. Fukagawa. 2013. The CCAN recruits CENP-A to the centromere and forms the structural core for kinetochore assembly. *J. Cell Biol.* 200:45–60. http://dx.doi.org/10.1083/jcb.201210106

Hornung, P., P. Troc, F. Malvezzi, M. Maier, Z. Demianova, T. Zimniak, G. Litos, F. Lampert, A. Schleiffer, M. Brunner, et al. 2014. A cooperative mechanism drives budding yeast kinetochore assembly downstream of CENP-A. *J. Cell Biol.* 206:509–524. http://dx.doi.org/10.1083/jcb.201403081

Izuta, H., M. Ikeno, N. Suzuki, T. Tomonaga, N. Nozaki, C. Obuse, Y. Kisu, N. Goshima, F. Nomura, N. Nomura, and K. Yoda. 2006. Comprehensive analysis of the ICEN (Interphase Centromere Complex) components enriched in the CENP-A chromatin of human cells. *Genes Cells.* 11:673–684. http://dx.doi.org/10.1111/j.1365-2443.2006.00969.x

Kato, H., J. Jiang, B.R. Zhou, M. Rozendaal, H. Feng, R. Ghirlando, T.S. Xiao, A.F. Straight, and Y. Bai. 2013. A conserved mechanism for centromeric nucleosome recognition by centromere protein CENP-C. *Science.* 340:1110–1113. http://dx.doi.org/10.1126/science.1235532

Kim, S., and H. Yu. 2015. Multiple assembly mechanisms anchor the KMN spindle checkpoint platform at human mitotic kinetochores. *J. Cell Biol.* 208:181–196. http://dx.doi.org/10.1083/jcb.201407074

Krizaic, I., S.J. Williams, P. Sánchez, M. Rodríguez-Corsino, P.T. Stukenberg, and A. Losada. 2015. The distinct functions of CENP-C and CENP-T/W in centromere propagation and function in *Xenopus* egg extracts. *Nucleus.* 6:133–143. http://dx.doi.org/10.1080/19491034.2014.1003509

Liu, S.T., J.B. Rattner, S.A. Jablonski, and T.J. Yen. 2006. Mapping the assembly pathways that specify formation of the trilaminar kinetochore plates in human cells. *J. Cell Biol.* 175:41–53. http://dx.doi.org/10.1083/jcb.200606020

Logsdon, G.A., E.J. Barrey, E.A. Bassett, J.E. DeNizio, L.Y. Guo, T. Panchenko, J.M. Dawicki-McKenna, P. Heun, and B.E. Black. 2015. Both tails and the centromere targeting domain of CENP-A are required for centromere establishment. *J. Cell Biol.* 208:521–531. http://dx.doi.org/10.1083/jcb.201412011

Maiolica, A., D. Cittaro, D. Borsotti, L. Sennels, C. Ciferri, C. Tarricone, A. Musacchio, and J. Rappsilber. 2007. Structural analysis of multiprotein complexes by cross-linking, mass spectrometry, and database searching. *Mol. Cell. Proteomics.* 6:2200–2211. http://dx.doi.org/10.1074/mcp.M700274-MCP200

Malvezzi, F., G. Litos, A. Schleiffer, A. Heuck, K. Mechtler, T. Clausen, and S. Westermann. 2013. A structural basis for kinetochore recruitment of the Ndc80 complex via two distinct centromere receptors. *EMBO J.* 32:409–423. http://dx.doi.org/10.1038/emboj.2012.356

Matson, D.R., P.B. Demirel, P.T. Stukenberg, and D.J. Burke. 2012. A conserved role for COMA/CENP-H/I/N kinetochore proteins in the spindle checkpoint. *Genes Dev.* 26:542–547. http://dx.doi.org/10.1101/gad.184184.111

McAinsh, A.D., and P. Meraldi. 2011. The CCAN complex: linking centromere specification to control of kinetochore-microtubule dynamics. *Semin. Cell Dev. Biol.* 22:946–952. http://dx.doi.org/10.1016/j.semcdb.2011.09.016

McCleland, M.L., M.J. Kallio, G.A. Barrett-Wilt, C.A. Kestner, J. Shabanowitz, D.F. Hunt, G.J. Gorbsky, and P.T. Stukenberg. 2004. The vertebrate Ndc80 complex contains Spc24 and Spc25 homologs, which are required to establish and maintain kinetochore-microtubule attachment. *Curr. Biol.* 14:131–137. http://dx.doi.org/10.1016/j.cub.2003.12.058

McClelland, S.E., S. Borusu, A.C. Amaro, J.R. Winter, M. Belwal, A.D. McAinsh, and P. Meraldi. 2007. The CENP-A NAC/CAD kinetochore complex controls chromosome congression and spindle bipolarity. *EMBO J.* 26:5033–5047. http://dx.doi.org/10.1038/sj.emboj.7601927

Milks, K.J., B. Moree, and A.F. Straight. 2009. Dissection of CENP-C-directed centromere and kinetochore assembly. *Mol. Biol. Cell.* 20:4246–4255. http://dx.doi.org/10.1091/mbc.E09-05-0378

Moree, B., C.B. Meyer, C.J. Fuller, and A.F. Straight. 2011. CENP-C recruits M18BP1 to centromeres to promote CENP-A chromatin assembly. *J. Cell Biol.* 194:855–871. http://dx.doi.org/10.1083/jcb.201106079

Nishino, T., K. Takeuchi, K.E. Gascoigne, A. Suzuki, T. Hori, T. Oyama, K. Morikawa, I.M. Cheeseman, and T. Fukagawa. 2012. CENP-T-W-S-X forms a unique centromeric chromatin structure with a histone-like fold. *Cell.* 148:487–501. http://dx.doi.org/10.1016/j.cell.2011.11.061

Nishino, T., F. Rago, T. Hori, K. Tomii, I.M. Cheeseman, and T. Fukagawa. 2013. CENP-T provides a structural platform for outer kinetochore assembly. *EMBO J.* 32:424–436. http://dx.doi.org/10.1038/emboj.2012.348

Obuse, C., H. Yang, N. Nozaki, S. Goto, T. Okazaki, and K. Yoda. 2004. Proteomics analysis of the centromere complex from HeLa interphase cells: UV-damaged DNA binding protein 1 (DDB-1) is a component of the CEN-complex, while BMI-1 is transiently co-localized with the centromeric region in interphase. *Genes Cells.* 9:105–120. http://dx.doi.org/10.1111/j.1365-2443.2004.00705.x

Okada, M., I.M. Cheeseman, T. Hori, K. Okawa, I.X. McLeod, J.R. Yates III, A. Desai, and T. Fukagawa. 2006. The CENP-H-I complex is required for the efficient incorporation of newly synthesized CENP-A into centromeres. *Nat. Cell Biol.* 8:446–457. http://dx.doi.org/10.1038/ncb1396

Okada, M., K. Okawa, T. Isobe, and T. Fukagawa. 2009. CENP-H-containing complex facilitates centromere deposition of CENP-A in cooperation with FACT and CHD1. *Mol. Biol. Cell.* 20:3986–3995. http://dx.doi.org/10.1091/mbc.E09-01-0065

Petrovic, A., S. Pasqualato, P. Dube, V. Krenn, S. Santaguida, D. Cittaro, S. Monzani, L. Massimiliano, J. Keller, A. Tarricone, et al. 2010. The MIS12 complex is a protein interaction hub for outer kinetochore assembly. *J. Cell Biol.* 190:835–852. http://dx.doi.org/10.1083/jcb.201002070

Petrovic, A., S. Mosalaganti, J. Keller, M. Mattiuzzo, K. Overlack, V. Krenn, A. De Antoni, S. Wohlgemuth, V. Cecatiello, S. Pasqualato, et al. 2014. Modular assembly of RWD domains on the Mis12 complex underlies outer kinetochore organization. *Mol. Cell.* 53:591–605. http://dx.doi.org/10.1016/j.molcel.2014.01.019

Przewloka, M.R., Z. Venkei, V.M. Bolanos-Garcia, J. Debski, M. Dadlez, and D.M. Glover. 2011. CENP-C is a structural platform for kinetochore assembly. *Curr. Biol.* 21:399–405. http://dx.doi.org/10.1016/j.cub.2011.02.005

Rago, F., K.E. Gascoigne, and I.M. Cheeseman. 2015. Distinct organization and regulation of the outer kinetochore KMN network downstream of CENP-C and CENP-T. *Curr. Biol.* 25:671–677. http://dx.doi.org/10.1016/j.cub.2015.01.059

Ribeiro, S.A., P. Vagnarelli, Y. Dong, T. Hori, B.F. McEwen, T. Fukagawa, C. Flors, and W.C. Earnshaw. 2010. A super-resolution map of the vertebrate kinetochore. *Proc. Natl. Acad. Sci. USA.* 107:10484–10489. http://dx.doi.org/10.1073/pnas.1002325107

Saitoh, H., J. Tomkiel, C.A. Cooke, H. Ratrie III, M. Maurer, N.F. Rothfield, and W.C. Earnshaw. 1992. CENP-C, an autoantigen in scleroderma, is a component of the human inner kinetochore plate. *Cell.* 70:115–125. http://dx.doi.org/10.1016/0092-8674(92)90538-N

Santaguida, S., and A. Musacchio. 2009. The life and miracles of kinetochores. *EMBO J.* 28:2511–2531. http://dx.doi.org/10.1038/emboj.2009.173

Schittenhelm, R.B., S. Heeger, F. Althoff, A. Walter, S. Heidmann, K. Mechtler, and C.F. Lehner. 2007. Spatial organization of a ubiquitous eukaryotic kinetochore protein network in *Drosophila* chromosomes. *Chromosoma.* 116:385–402. http://dx.doi.org/10.1007/s00412-007-0103-y

Schleiffer, A., M. Maier, G. Litos, F. Lampert, P. Hornung, K. Mechtler, and S. Westermann. 2012. CENP-T proteins are conserved centromere receptors of the Ndc80 complex. *Nat. Cell Biol.* 14:604–613. http://dx.doi.org/10.1038/ncb2493

Screpanti, E., A. De Antoni, G.M. Alushin, A. Petrovic, T. Melis, E. Nogales, and A. Musacchio. 2011. Direct binding of Cenp-C to the Mis12 complex joins the inner and outer kinetochore. *Curr. Biol.* 21:391–398. http://dx.doi.org/10.1016/j.cub.2010.12.039

Song, K., B. Gronemeyer, W. Lu, E. Eugster, and J.E. Tomkiel. 2002. Mutational analysis of the central centromere targeting domain of human centromere protein C, (CENP-C). *Exp. Cell Res.* 275:81–91. http://dx.doi.org/10.1006/excr.2002.5495

Sugimoto, K., K. Kuriyama, A. Shibata, and M. Himeno. 1997. Characterization of internal DNA-binding and C-terminal dimerization domains of human centromere/kinetochore autoantigen CENP-C in vitro: role of DNA-binding and self-associating activities in kinetochore organization. *Chromosome Res.* 5:132–141. http://dx.doi.org/10.1023/A:1018422325569

Suzuki, A., B.L. Badger, X. Wan, J.G. DeLuca, and E.D. Salmon. 2014. The architecture of CCAN proteins creates a structural integrity to resist spindle forces and achieve proper Intrakinetochore stretch. *Dev. Cell.* 30:717–730. http://dx.doi.org/10.1016/j.devcel.2014.08.003

Tachiwana, H., S. Müller, J. Blümer, K. Klare, A. Musacchio, and G. Almouzni. 2015. HJURP involvement in de novo $CenH3^{CENP-A}$ and CENP-C recruitment. *Cell Reports.* 11:22–32. http://dx.doi.org/10.1016/j.celrep.2015.03.013

Takeuchi, K., T. Nishino, K. Mayanagi, N. Horikoshi, A. Osakabe, H. Tachiwana, T. Hori, H. Kurumizaka, and T. Fukagawa. 2014. The centromeric nucleosome-like CENP-T-W-S-X complex induces positive supercoils into DNA. *Nucleic Acids Res.* 42:1644–1655. http://dx.doi.org/10.1093/nar/gkt1124

Tanaka, K., H.L. Chang, A. Kagami, and Y. Watanabe. 2009. CENP-C functions as a scaffold for effectors with essential kinetochore functions in mitosis and meiosis. *Dev. Cell.* 17:334–343. http://dx.doi.org/10.1016/j.devcel.2009.08.004

Tighe, A., V.L. Johnson, and S.S. Taylor. 2004. Truncating APC mutations have dominant effects on proliferation, spindle checkpoint control, survival and chromosome stability. *J. Cell Sci.* 117:6339–6353. http://dx.doi.org/10.1242/jcs.01556

Trazzi, S., G. Perini, R. Bernardoni, M. Zoli, J.C. Reese, A. Musacchio, and G. Della Valle. 2009. The C-terminal domain of CENP-C displays multiple and critical functions for mammalian centromere formation. *PLoS ONE.* 4:e5832. http://dx.doi.org/10.1371/journal.pone.0005832

Unhavaithaya, Y., and T.L. Orr-Weaver. 2013. Centromere proteins CENP-C and CAL1 functionally interact in meiosis for centromere clustering, pairing, and chromosome segregation. *Proc. Natl. Acad. Sci. USA.* 110:19878–19883. http://dx.doi.org/10.1073/pnas.1320074110

Yang, C.H., J. Tomkiel, H. Saitoh, D.H. Johnson, and W.C. Earnshaw. 1996. Identification of overlapping DNA-binding and centromere-targeting domains in the human kinetochore protein CENP-C. *Mol. Cell. Biol.* 16:3576–3586.